Submission code: V8MXP6QZWM

See this and other abstracts on our website: https://home.sbgf.org.br/Pages/resumos.php

Application of different acquisition geometries in refraction tomography

Daniel Da Silva Ferreira (GISIS/UFF), Luiz Alberto Santos (PETROBRAS), Marcos Lopes (GISIS/UFF), Marco Cetale (GISIS/UFF)

Application of different acquisition geometries in refraction tomography

This paper was prepared for presentation during the 19th International Congress of the Brazilian Geophysical Society held in Rio de Janeiro, Brazil, 18-20 November 2025. Contents of this paper were reviewed by the Technical Committee of the 19th International Congress of the Brazilian Geophysical Society and do not necessarily represent any position of the SBGf, its officers or members.

Abstract Summary

The final product of seismic data processing is directly related to the velocity model used, which can be obtained through several techniques, including seismic refraction tomography. We evaluated the effect of acquisition geometry on the tomographic results in seismic refraction data. Based on studies in the Volta Redonda, Resende, and Taubaté basins, a model with pinchout was built and four distinct acquisition geometries were applied. The best inversion result was obtained with the full-spread geometry, which had the highest number of shots and receivers placed on the surface, presenting the highest convergence rate among the tests.

Introduction

The final quality of processed seismic images is essentially related to the subsurface velocity model (Almeida, 2013). This can be accurately obtained through geophysical profiles; however, these are specific and costly measures. A way to obtain a velocity model quickly, inexpensively, and with high accuracy compared to other costly techniques is seismic tomography (Bulhões, 2020). Among tomographic techniques, refraction tomography, in which the only data used are first arrival times (first break), can provide accurate velocity models, especially at shallow depths.

In this context, the objective of this study is to verify the influence of acquisition geometry on the tomographic inversion results in seismic refraction data. To achieve this, a velocity model with a pinchout was created, based on structures present at the edges of the Resende, Volta Redonda, and Taubaté basins, which belong to the central part of the Southeastern Brazilian Continental Rift (RCSB) (Figure 1). Four types of acquisition geometry were considered: end-on spread, split-spread, roll-along of the source (with fixed receivers in the central part of the model) and full-spread (with sources and receivers distributed across the entire surface of the model). The first shot of all tests was located 10 m from the left edge and 1 m in depth. In the case of the end-on and split-spread geometries, a roll was performed for each shot. Other acquisition parameters for each survey can be found in Table 1.

Parameters	End-on spread	Split spread	Roll-along of the source	Full-spread
Number of shots	77	78	149	149
Shot interval	10 m	10 m	10 m	10 m
Number of receivers	72	72	72	149
Interval between receivers	10 m	10 m	10 m	10 m
Minimum/Maximum offset	10 m / 720 m	10 m / 360 m	10 m / 720 m	10 m / 1480 m

Table 1: Acquisition parameters of each seismic survey.

Method and/or Theory

After the construction of the velocity model, inspired by terrestrial basins of Resende, Volta Redonda and Taubaté, synthetic data for direct and refracted wave travel times were generated in a synthetic seismic survey. The travel time at each point in space is calculated using the Eikonal equation (Eq. 1), which can be represented by

$$s^2(\mathbf{X}) = (\nabla \mathbf{T})^2, \tag{1}$$

where s is the slowness field, X = (x, z) is the position vector, and the function T represents the travel time at each point in space when the equation is solved.

Podvin and Lecomte (1991) developed an algorithm that uses the finite difference method to find an approximate solution to the Eikonal equation, in which the travel times of first arrivals are calculated. These times are obtained based on Fermat's Principle, which establishes that the wave travels along the path of least time.

After obtaining the travel times, ray tracing can then be applied. Each traced ray represents the trajectory of the first arrival of a wave traveling from a source to a given receiver (Almeida, 2013). When traced, the ray follows the opposite direction of the travel time gradient, from the receiver to the source (Vidale, 1988). For refraction tomography, only first arrival times are needed; therefore, the trajectories of the waves that reach the receivers first are represented by traced rays.

The primary objective of ray tracing is to generate the Fréchet derivatives to obtain the sensitivity matrix, from which it is possible to observe which regions of the model are densely covered by the rays (greater coverage) and, consequently, will provide a better response to tomography (Almeida, 2013). Nonlinear inversion and the L_2 norm were used to minimize the following objective function:

$$\Phi(\mathbf{m}) = \|\mathbf{d} - \mathbf{G}(\mathbf{m})\|_2^2 + \lambda \|\mathbf{L}\mathbf{m}\|_2^2, \tag{2}$$

where d corresponds to the observed data, G(m) to calculated data for the current model m, λ is the regularization parameter, and L is a discrete derivative operator, which in this study is a second-order derivative operator stabilizing the inversion scheme (second-order Tikhonov regularization). According to (Bulhões, 2020), in first-arrival tomography, second-order Tikhonov regularization exhibits rapid convergence.

At each iteration of the tomography, a linear system is solved. In order to avoid matrix inversion, a special type of conjugate gradient method was applied to solve the least squares problem. This method calculates the solution of $Ax = b$ without the need to calculate the Hessian matrix (Hestenes et al., 1952). Thus, the problem to be solved iteratively is given by:

$$\mathbf{A}^T \mathbf{A} \Delta \mathbf{m} = \mathbf{A}^T \Delta \mathbf{d}, \tag{3}$$

where A is the sensitivity matrix containing the Fréchet derivatives and the second-order Tikhonov regularization operator, Δm is the variation of the velocity model and Δd is the difference between calculated and observed data.

In this study, no tolerance term was used. Instead, the convergence criterion was defined as a total number of 10 iterations. To reduce artifacts caused by poor illumination, a Gaussian smoothing filter was also applied between iterations. The complete workflow of the tomographic can be seen in Figure 2.

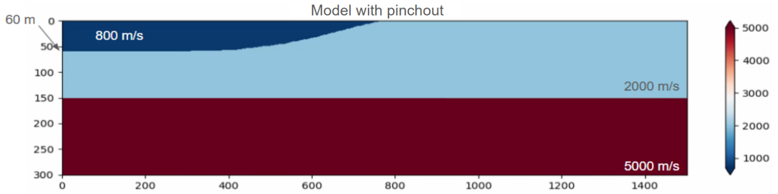

Figure 1: Reference model.

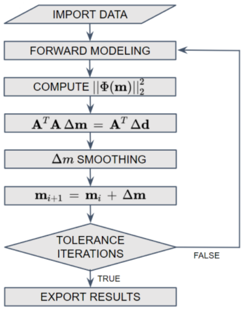

Figure 2: General workflow of classical tomographic inversion.

Results

As results, Figure 3 presents the comparison between the inverted models generated from the four acquisition geometries adopted in this study. To assist in quality control, this figure includes the convergence curves corresponding to the four tests conducted according to the methodology described. It should be emphasized that only the inversion result within the white dashed lines is reliable. Among the tests performed, the lowest residual was observed with the end-on acquisition geometry. However, the highest convergence rate was found in the full-spread geometry test, demonstrating greater geological realism in the deeper part and recovering the pinchout structure in the shallow part. Except for the split-spread test, the other tests produced anomalous structures in the middle and deep parts of the model due to inadequate illumination for inversion. Despite the velocity artifacts generated, all four geometries allowed for an appropriate estimation of the model in the shallow part, as they enabled the recovery of the pinchout structure.

Conclusions

The evaluation of the effect of acquisition geometry on tomographic inversion of refractions and diving waves illustrates that, despite the higher absolute residual, the richness of receivers in the full-spread survey provides greater convergence and lower relative residual. This provided greater geological realism in the deeper part. Nevertheless, the end-on spread, split-spread, and roll-along of the source geometries allow for the estimation of the velocity model in the shallow part.

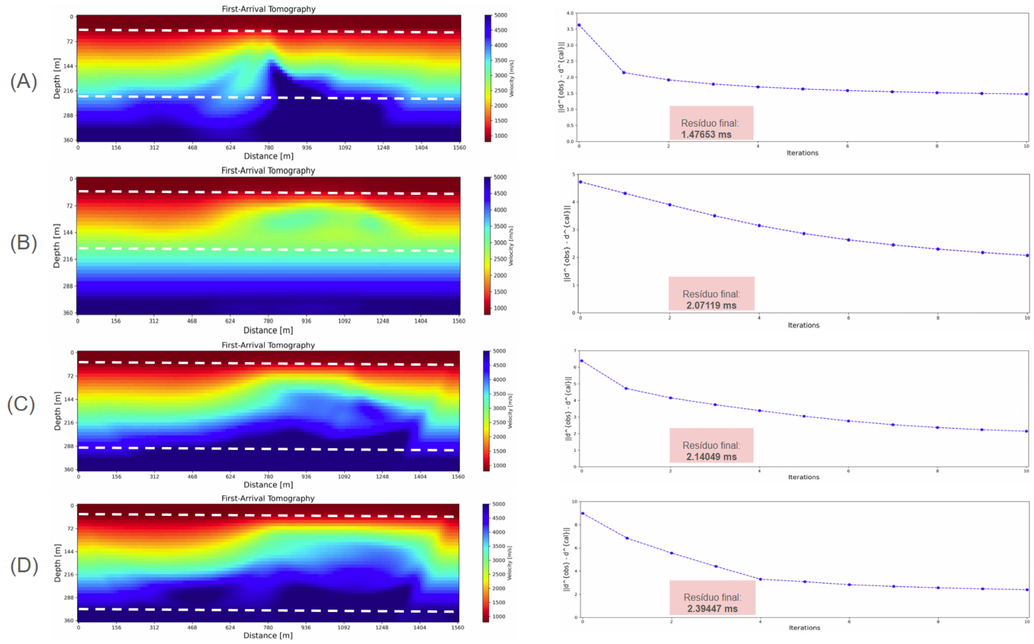

Figure 3: Inverted models and convergence curves for the four adopted acquisition geometries.

Acknowledgments

The authors from Fluminense Federal University acknowledge the financial support from Petrobras through the R&D project Tectônica Cenozoica da Margem Continental do Sudeste do Brasil: padrões de deformação e controle na sedimentação (ANP nº 22969-0). The strategic importance of the R&D levy regulation of the National Agency for Petroleum, Natural Gas and Biofuels (ANP) is gratefully appreciated. We would like to thank Mr. Rodrigo Stern (GISIS/UFF) for the IT support.

References

Almeida, V. T. X. d.; SANTOS, M. A. C., 2013, Tomografia sísmica de superfície: modelagem direta calculando as trajetórias de ondas refratadas: Dissertação (mestrado em geofísica), Universidade Federal Fluminense (UFF), Niterói, Brasil.

Bulhões, F. C., 2020, Efeitos da regularização na tomografia de refração: Dissertação (mestrado em geofísica), Universidade Federal Fluminense (UFF), Niterói, Brasil.

Hestenes, M. R., E. Stiefel, and et al., 1952, Methods of conjugate gradients for solving linear systems: Journal of research of the National Bureau of Standards, **49**, 409–436.

Podvin, P., and I. Lecomte, 1991, Finite difference computation of traveltimes in very contrasted velocity models: a massively parallel approach and its associated tools: Geophysical Journal International, **105(1)**, 271–284.

Vidale, J., 1988, Finite-difference calculation of travel times: Bulletin of the seismological society of America, **78**, 2062–2076.